SLD PHYSICS NOTE NO. 013

FG05-91ER40627

CONF-920532--38

A Study of Energy-Energy Correlations and Measurement of α_s at the Z^0 Resonance

CONF-920837--38

DE93 005894

The SLD Collaboration

Contributed to the XXVI International Conference on High Energy Physics
Dallas, USA, August 6-12, 1992

ABSTRACT

We present the energy-energy correlation (EEC) distribution and its asymmetry ($AEEC$) in hadronic decays of Z^0 bosons measured by the SLD at SLAC. The data are found to be in good agreement with the predictions of perturbative QCD and fragmentation Monte Carlo models of hadron production. After correction for hadronization effects the data are compared with $\mathcal{O}(\alpha_s^2)$ perturbative QCD calculations from various authors. Fits to the central region of the EEC yield substantially different values of the QCD scale $\Lambda_{\overline{MS}}$ for each of the QCD calculations. There is also a sizeable dependence of the fitted $\Lambda_{\overline{MS}}$ value on the QCD renormalization scale factor, f. Our preliminary results are $\alpha_s(M_Z) = 0.121 \pm 0.002(stat.) \pm 0.004(exp.sys.)^{+0.016}_{-0.009}(theor.)$ for EEC and $\alpha_s(M_Z) = 0.108 \pm 0.003(stat.) \pm 0.005(exp.sys.)^{+0.008}_{-0.003}(theor.)$ for $AEEC$. The largest contribution to the error arises from the theoretical uncertainty in choosing the QCD renormalization scale.

1. Introduction

The SLAC Linear Collider (SLC) produces electron-positron annihilation events at the Z^0 resonance which are recorded by the SLC Large Detector (SLD) [1]. The SLC/SLD project enjoyed a successful engineering run in 1991; in addition to commissioning the SLD, studies were made of the properties of hadronic decays of Z^0 bosons, resulting in preliminary measurements of the strong coupling α_s [2]. The first physics run began in February 1992, during which the SLC performance has continued to improve, routinely achieving Z^0 production rates of 10-20 per hour. Up to the end of July a sample of 8,000 Z^0s had been accumulated by the SLD; approximately 6,000 of these events were used for the analysis presented here.

A major achievement of the 1992 run has been the delivery of an intense beam of longitudinally polarized electrons#1 and the observation of decays of the resulting Z^0s. Details of the polarization production and measurement system are contributed to this conference [3], as well as preliminary measurements [4] of the left-right cross-section asymmetry [5].

The energy-energy correlations (EEC) distribution for hadronic events in e^+e^- annihilation, and its asymmetry ($AEEC$), were introduced by Basham *et al.* [6] as good experimental observables for a precise test of QCD. Since then, most e^+e^- experimental groups [7,8,9,10,11,12] have used them to determine the strong coupling α_s.

In this paper, we present measurements of the EEC and $AEEC$ distributions from hadronic Z^0 decay events collected by SLD and determine α_s by fitting the $\mathcal{O}(\alpha_s^2)$ QCD formulae to the parton-level corrected EEC and $AEEC$ distributions. Further details of comparison of the event shape observables from hadronic decays of Z^0's produced by polarized and unpolarized electron beams are given in separate contributions to this conference [13].

2. The SLD

The detector is shown schematically in Fig. 1 and a detailed outline of its construction and performance is described in [1]. The micro-vertex detector (VXD) and Cherenkov Ring Imaging Detectors (CRID) were not used in this analysis, but are described in separate contributions to this conference [14].

Charged particles are tracked in the Central Drift Chamber (CDC) which consists of 10 superlayers, each containing 8 layers of axial or stereo sense wires. Tracking is extended to forward angles (10° from the beam axis) by endcap drift chambers. Momentum measurement is provided by a uniform axial magnetic field of 0.6T.

Particle energies are measured in the Liquid Argon Calorimeter (LAC) [15], which contains both electromagnetic and hadronic sections, and in the Warm Iron Calorimeter [16], which forms the outer layer of the hadronic calorimetry and also provides tracking for muons. The LAC is segmented into approximately 40,000 projective

#1 An electron beam polarization of ~ 22% has been achieved to date.

towers and has a resolution of about 15% for the measured Z^0 mass. Luminosity is measured from the rate of small-angle Bhabha events detected in forward silicon-tungsten calorimeters [17] mounted close to the beampipe.

3. Triggering and Data Selection

Two independent triggers were used for hadronic events: an energy trigger requiring a total LAC energy in excess of 8 GeV, and a charged track trigger requiring at least two well-separated tracks in the CDC. The trigger for Bhabha events required typically 10 GeV in both forward and backward luminosity monitors.

A loose selection of hadronic events was then made by two independent methods: one based on the topology of energy depositions in the LAC, the other on the number and topology of charged tracks measured in the CDC. After statistical subtraction of backgrounds, comparison of the number of hadronic events with the number of luminosity Bhabha events indicated a combined triggering and selection efficiency for hadronic events of better than 90% for the LAC method. 99% of the events identified by the CDC method were also identified by the LAC method. The residual contamination in this overlap sample was estimated to be mainly from τ-pair events, calculated to be at the level of 0.3%.

The analysis presented here used charged tracks measured in the CDC. A set of cuts was applied to the data to select well-measured tracks and events well-contained within the detector acceptance. Tracks were required to have:

- a fit quality of $\sqrt{2\chi^2_{fit}} - \sqrt{2N_{df} - 1} < 15$, where N_{df} is the number of degrees of freedom for the track fit
- a closest approach to the beam axis within 10 cm and within 20 cm along the beam axis of the nominal interaction point
- a polar angle, θ, with respect to the beam axis with $|\cos\theta| < 0.80$
- a minimum momentum transverse to this axis of $p_\perp > 150$ MeV/c^2.

Events were required to have:

- a minimum of five such tracks
- no track with a momentum larger than 100 GeV
- a thrust axis direction, θ_T, within $|\cos\theta_T| < 0.71$
- a minimum charged visible energy greater than 0.2M$_Z$, where all tracks were assigned the charged pion mass.

After applying these cuts, distributions of track multiplicity, polar angle, momenta and event θ_T and E_{vis} were reproduced by Monte Carlo simulations. 3837 events survived these cuts, of which 3163 were produced by left- or right-polarized electron beams and the remainder by unpolarized beams. We combined both event samples in this analysis. The total residual contamination from background sources was estimated to be negligible.[#2]

4. Measurement of the Energy-Energy Correlations

Experimentally, the EEC is defined as the normalized, energy-weighted sum over all pairs of particles whose opening angles, χ_{ij}, lie between $\chi - \Delta\chi/2$ and $\chi + \Delta\chi/2$:

$$EEC(\chi) = \frac{1}{N_{event}} \sum_{1}^{N_{event}} \left(\frac{1}{2\Delta\chi} \int_{\chi-\frac{\Delta\chi}{2}}^{\chi+\frac{\Delta\chi}{2}} \sum_{i,j=1}^{n_{particle}} \frac{E_i E_j}{E_{vis}^2} \delta(\chi' - \chi_{ij}) d\chi' \right) \tag{4.1}$$

where χ is an opening angle to be studied for the correlations, $\Delta\chi$ is a bin width, E_i and E_j are the energies of particles i and j and E_{vis} is the sum of the energies of all particles in the event. Note that E_{vis} is used to normalize the particle energies instead of $\sqrt{s}$ so that the EEC is less sensitive to undetected particles and $\int EEC(\chi)d\chi = 1$ is ensured.

The asymmetry of the EEC is defined as

$$AEEC(\chi) = EEC(\pi - \chi) - EEC(\chi) \tag{4.2}$$

The perturbative contributions of hard gluon emissions to the EEC are asymmetric, so that the $AEEC$ is expected to be more sensitive to α_s [6].

Perturbative QCD calculations of the EEC have been performed to $\mathcal{O}(\alpha_s^2)$ by Richards, Stirling and Ellis (RSE) [18], Ali and Barreiro (AB) [19], Falck and Kramer (FK) [20] and Kunzst and Nason (KN) [21]. The EEC can be written in the form:

$$EEC(\chi) = \frac{\alpha_s(\mu)}{2\pi} A(\chi) + \left(\frac{\alpha_s(\mu)}{2\pi}\right)^2 [A(\chi) 2\pi b_0 \ln(\mu^2/s) + B(\chi)] \tag{4.3}$$

where $\alpha_s(\mu)$ is related to the QCD scale $\Lambda_{\overline{MS}}$ by [22]:

$$\alpha_s(\mu) = \frac{12\pi}{(33 - 2n_f)\ln(\mu^2/\Lambda^2_{\overline{MS}})} \left[1 - \frac{6(153 - 19n_f)}{(33 - 2n_f)^2} \frac{\ln[\ln(\mu^2/\Lambda^2_{\overline{MS}})]}{\ln(\mu^2/\Lambda^2_{\overline{MS}})} \right] \tag{4.4}$$

The first order coefficients $A(\chi)$ can be calculated analytically and the second order coefficients $B(\chi)$ are calculated numerically. μ is the renormalization scale, $b_0 = (33 - 2n_f)/12\pi$, where n_f is the number of active flavors, and $s = E^2_{CM}$. The main difference between the theoretical calculations mentioned above is in the method used

#2 Beam-related backgrounds are discussed in [4].

to treat the singularities found in calculating the second order coefficient. Another difference is the choice of renormalization scale μ. RSE, AB and FK set μ to $\sqrt{s}$ in estimating the second order term. On the other hand, KN keep the $\ln(\mu^2/s)$ term in the second order coefficient in equation (4.3) so that the renormalization scale μ can be treated as a free parameter in their calculation. We keep an explicit μ dependence for the RSE, AB and FK cases in equation (4.3). It is important to notice that $\mathcal{O}(\alpha_s^2)$ perturbative QCD calculations do not specify the μ value to be used in any physical observable [21], although this scale ambiguity will presumably vanish if the calculation is done to all orders of the perturbation series. Equation (4.3) is best suited to study the renormalization scale dependence of $\Lambda_{\overline{MS}}$ in the EEC analysis. We note that several theoretical approaches have been proposed to fix or optimize the renormalization scale in the framework of $\mathcal{O}(\alpha_s^2)$ perturbative QCD [23,24,25,26]. Here we treat μ as a free parameter.

Fig. 2 shows the preliminary measured EEC and $AEEC$ distributions at the detector level as points with error bars. The solid histograms represent the result from the JETSET 6.3 [27] parton shower Monte Carlo program with initial state photon radiation, followed by detector simulation, and the same event reconstruction program and event analysis cuts as used for the data. The dashed histograms show the corresponding result for the HERWIG 5.3 [28] parton shower program, using the same procedures. For each program, 10,000 events were generated. We used parameter values of the JETSET 6.3 Monte Carlo event generator determined by the TASSO Collaboration at $\sqrt{s}$=35 GeV [29], which have been found to be in good agreement with Z^0 data [30]; these are listed in Table 1. For the HERWIG 5.3 Monte Carlo we used the default parameter values which were derived from comparisons with LEP data [31].

After detector simulation, both JETSET 6.3 and HERWIG 5.3 reproduce the measured distributions as shown in Fig. 2. We therefore used these simulations to correct our data for the effects of initial state photon radiation, detector acceptance and resolution, interactions, decays, analysis cuts and unmeasured neutral particles. The EEC distribution was corrected to the hadron level by applying bin-by-bin correction factors, $C_{det}(\chi_i)$:

$$EEC_{hadron}(\chi_i) = C_{det}(\chi_i) \times EEC_{meas}(\chi_i), \tag{4.5}$$

where the correction factors were estimated by comparing Monte Carlo results before and after detector simulation:

$$C_{det}(\chi_i) = \frac{EEC^{MC}_{hadron}(\chi_i)}{EEC^{MC}_{detector}(\chi_i)}, \tag{4.6}$$

where $EEC^{MC}_{detector}(\chi_i)$ represents the histogram content at bin χ_i of the EEC obtained from the charged particles of the reconstructed Monte Carlo events. The corrected $AEEC$ is then derived from the corrected EEC. The correction factors for the EEC determined using the JETSET 6.3 Monte Carlo are shown in Fig. 3.

The statistical errors on the EEC and $AEEC$ distributions have strong bin-to-bin correlations because each event contributes to several neighboring bins. There is no straightforward way to evaluate these correlations. In order to estimate the statistical errors, we generated 10 different event samples using the JETSET 6.3 Monte Carlo, each with the same number of events as the data sample. Then we constructed the 10 sets of EEC and $AEEC$ distributions from these event samples and set the statistical errors in each bin to be equal to the root-mean-square deviation in that bin.

5. Determination of $\Lambda_{\overline{MS}}$ and α_s

5.1 Determination of the QCD scale $\Lambda_{\overline{MS}}$

In order to determine the value of $\Lambda_{\overline{MS}}$, we corrected the data further to the parton level and compared them with the $\mathcal{O}(\alpha_s^2)$ theoretical formulae calculated by RSE, AB, FK and KN.

The correction method is essentially the same as discussed in the previous section and it is again performed by applying bin-by-bin correction factors which are derived from JETSET 6.3:

$$EEC_{parton}(\chi_i) = C_{frag}(\chi_i) \times EEC_{hadron}(\chi_i). \tag{5.1}$$

The correction factor $C_{frag}(\chi_i)$ is defined by:

$$C_{frag}(\chi_i) = \frac{EEC^{MC}_{parton}(\chi_i)}{EEC^{MC}_{hadron}(\chi_i)}, \tag{5.2}$$

where $EEC^{MC}_{hadron}(\chi_i)$ is the hadron level EEC as defined in Section 4 and $EEC^{MC}_{parton}(\chi_i)$ is the content of bin χ_i constructed at the parton level, with an invariant mass cutoff for the parton shower of Q_0=1.0GeV/c^2. The corrected $AEEC$ is again derived from the corrected EEC.

In Fig. 4 the correction factors for fragmentation effects are shown. They are nearly flat with a maximum of 10% deviation from their mean in the central angular region $35° < \chi < 145°$. Emission of hard gluons dominates in the central angular region of the EEC distribution so that this region is especially sensitive to α_s.

Using equations (4.3) and (4.4), we performed a one-parameter fit of each of the four $\mathcal{O}(\alpha_s^2)$ analytical formulae to the corrected EEC distributions in the angular region of $36.0° - 144.0°$ to determine $\Lambda_{\overline{MS}}$. As mentioned in Section 4, the renormalization scale factor $f = \mu^2/s$ is not fixed in a $\mathcal{O}(\alpha_s^2)$ perturbative QCD calculation. We thus performed the fit after setting f to various values between 0.005 and 1.0. The same procedure was applied to the corrected $AEEC$ distributions in the angular range of $28.8° - 90.0°$. Note that FK define a pre-cluster before calculating their formula by applying a parton resolution parameter [20] y_{min}=0.0001, 0.001 and 0.01 whereas the RSE, AB and KN formulae are valid for $y_{min} = 0$ [12]. We take y_{min}=0.0001 to fit the FK formula to our data because this y_{min} value, which corresponds to $Q_0 \approx 1.0\mathrm{GeV/c^2}$, is small enough to be comparable with the other calculations.

In Fig. 5 the results of a fit, with the renormalization scale factor f=0.1, to the parton-level corrected *EEC* and *AEEC* are shown. Fig. 6 shows the fitted $\Lambda_{\overline{MS}}$ values as a function of the renormalization scale factor f for the four theoretical formulae from the *EEC* and *AEEC* respectively. The four QCD formulae give substantially different values of $\Lambda_{\overline{MS}}$. There is also a sizeable dependence of the fitted $\Lambda_{\overline{MS}}$ value on the renormalization factor f. As noted in Section 4, the *EEC* and the *AEEC* distributions have strong bin-to-bin correlations which are difficult to estimate. In order to estimate the statistical errors on $\Lambda_{\overline{MS}}$, we again made use of the previously generated 10 sets of JETSET 6.3 Monte Carlo events. We performed the same fitting procedure to the *EEC* and the *AEEC* for each of these sets and took the root-mean-square deviation of the 10 $\Lambda_{\overline{MS}}$ values thus determined as the statistical error of the fitted $\Lambda_{\overline{MS}}$.

5.2 Systematic errors in $\Lambda_{\overline{MS}}$

We took the $\Lambda_{\overline{MS}}$ value obtained from the KN formula with the renormalization scale factor f=0.1 as the central value of $\Lambda_{\overline{MS}}$ for both *EEC* and *AEEC* when we estimated the systematic errors in $\Lambda_{\overline{MS}}$.

The systematic uncertainties in $\Lambda_{\overline{MS}}$ can be divided into two categories. One contains the experimental systematic errors which arise from the limited acceptance, efficiency and resolution of the detector, and from biases due to the imperfections in detector simulation and in event reconstruction programs and due to selection criteria applied to the data for this analysis. The other encompasses the theoretical uncertainties which arise from the hadronization, and from the unknown higher order corrections to the theoretical calculations, in addition to uncertainties in the theoretical calculations themselves. Our study of experimental systematic errors is still in progress. We describe below preliminary results for those systematic effects which we have so far considered.

The experimental systematic errors were estimated by repeating the whole analysis for the event sets II and III defined by the cuts in Table 2. Then we took the full range of the $\Lambda_{\overline{MS}}$ values as twice the error. We found 52 MeV from the EEC and 26 MeV from the *AEEC* as this part of the experimental systematic error.

We also checked the deviation when the angular region used in the fit was changed. We varied the fitting region from $14.4° - 165.6°$ to $46.8° - 133.2°$ for the EEC and from $14.4° - 90.0°$ to $46.8° - 90.0°$ for the AEEC. We estimated the error to be 16 MeV and 26 MeV, taking the full range of the $\Lambda_{\overline{MS}}$ values as twice the error, from the *EEC* and *AEEC* respectively.

These two errors were added in quadrature to obtain the experimental systematic error.

The theoretical errors from the uncertainties in parton production and hadronization were estimated by repeating the analysis process from the hadron level corrected distributions. The *default* values of parameters, given in Table 1, for the parton shower (Λ_{QCD} and Q_0) and the fragmentation function (a, b and σ_q) in the JETSET6.3 Monte Carlo were used to derive the new correction factors for hadronization. The fitting procedure was applied again to the parton-level EEC and $AEEC$ corrected by these new correction factors. Then we took the deviation from the standard value of $\Lambda_{\overline{MS}}$ as the error and found 10 MeV and 16 MeV, from the EEC and $AEEC$ respectively.

Another contribution to the theoretical error arises from the differences among the four QCD calculations. Taking KN as the central value, the scatter in the $\Lambda_{\overline{MS}}$ values shown in Fig. 6 is: $^{+109}_{-76}$ MeV and $^{+57}_{-9}$ MeV, from the EEC and $AEEC$ respectively.

Finally, the renormalization scale ambiguities were estimated by taking the maximum deviation from the value of $\Lambda_{\overline{MS}}$ determined with f=0.1 for each of four QCD formulae when we changed the scale factor from 0.005 to 1.0 for both the EEC and the $AEEC$. For KN, this error was found to be $^{+200}_{-102}$ MeV and $^{+28}_{-10}$ MeV, from the EEC and $AEEC$ respectively. The variation is comparable for all four calculations. As we mentioned in Section 4, the $\mathcal{O}(\alpha_s^2)$ perturbative QCD calculations do not determine the renormalization scale. These errors may, therefore, be considered to be the uncertainties arising from the unknown higher order terms in perturbative QCD calculations.

5.3 Results

Taking the central values of $\Lambda_{\overline{MS}}$ from KN at f=0.1, we obtained:

$$EEC : \Lambda_{\overline{MS}} = 273 \pm 20(stat.) \pm 54(exp.sys.) \pm 10(had.)^{+109}_{-76}(calc.)^{+200}_{-102}(scale)\ \mathrm{MeV}$$
$$AEEC : \Lambda_{\overline{MS}} = 119 \pm 18(stat.) \pm 37(exp.sys.) \pm 16(had.)^{+57}_{-9}(calc.)^{+28}_{-10}(scale)\ \mathrm{MeV}$$

When these values were converted to $\alpha_s(M_Z)$ values, we obtained:

$$EEC : \alpha_s(M_Z) = 0.121 \pm 0.002(stat.) \pm 0.004(exp.sys.)^{+0.016}_{-0.009}(theor.)$$
$$AEEC : \alpha_s(M_Z) = 0.108 \pm 0.003(stat.) \pm 0.005(exp.sys.)^{+0.008}_{-0.003}(theor.)$$

The total theoretical systematic errors are the square root of the quadrature sum of the errors from hadronization, difference between the four theoretical calculations and ambiguity in the choice of renormalization scale.

Fig. 7 shows the $\alpha_s(M_Z)$ values from our analysis and those from similar LEP analyses [8,9,10,11,12]. Our $\alpha_s(M_Z)$ values are in good agreement with the LEP values within experimental errors and also with our values from a jet rate analysis [32]. Error bars with solid lines indicate the total experimental errors, which include statistical errors and experimental systematic errors; dashed lines indicate the theoretical errors. In general the errors are dominated by the theoretical ones.

6. Summary

We have studied the EEC and $AEEC$ distributions in hadronic Z^0 decays. We have determined $\Lambda_{\overline{MS}}$ and α_s values by comparing four $\mathcal{O}(\alpha_s^2)$ perturbative QCD calculations to parton-level corrected EEC and $AEEC$ distributions from our measurements. In order to estimate the theoretical uncertainties, we varied the renormalization scale factor $f = \mu^2/s$ from 0.005 to 1.0. Our preliminary results are $\alpha_s(M_Z) = 0.121 \pm 0.002(stat.) \pm 0.004(exp.sys.)^{+0.016}_{-0.009}(theor.)$ from the EEC and $\alpha_s(M_Z) = 0.108 \pm 0.003(stat.) \pm 0.005(exp.sys.)^{+0.008}_{-0.003}(theor.)$ from the $AEEC$. The total errors are dominated by the theoretical errors for both the EEC and the $AEEC$, although these depend upon the range chosen for variation of the renormalization scale. Our results are in good agreement with similar analyses at LEP.

Acknowledgements

The SLD Collaboration is indebted to all the SLAC staff whose efforts resulted in the successful operation of the SLC which produced the events used in this paper. We wish to thank G. Kramer and J.W. Gary for helpful comments relating to this analysis.

Table 1
The main parameters of the JETSET6.3 Monte Carlo with parton shower.

Parameter	Name	Default value	used value
Λ_{LLA}(GeV)	PARE(21)	0.4	0.26
Q_0(GeV/c^2)	PARE(22)	1.0	1.0
σ_q(GeV)	PAR(12)	0.35	0.39
a	PAR(31)	0.5	0.18
b(GeV^{-1})	PAR(32)	0.9	0.34

Table 2
Three sets of event selection criteria used to study the experimental systematic error in $\Lambda_{\overline{MS}}$. N_{good} is the number of well-measured tracks, E_{vis} is the charged visible energy and θ_T is the thrust axis direction.

Cut	Set I standard	Set II tight	Set III loose
N_{good}	≥5	≥7	≥5
$E_{vis}/\sqrt{s}$	>0.2	>0.25	>0.15
$\lvert\cos\theta_T\rvert$	<0.71	<0.71	<0.75
# of events	3,837	3,629	4,254

REFERENCES

1. SLD Design Report, SLAC Report 273 (1984).
2. SLD Collab., P.N. Burrows *et al.*, SLAC-Pub-5802 (1992).
3. SLD Collab., talk presented at this conference by N. Phinney.
4. SLD Collab., 'Measurement of the left-right cross section asymmetry in Z boson production at E_{cm}=91.4GeV', paper submitted to this conference and talk presented by P. Rowson.
5. See *eg.* CERN 88-06, Vol. 1, (1988), eds. G. Alexander *et al.*
6. C.L. Basham *et al.*, Phys. Rev. Lett. **41** (1978)1585, Phys. Rev. **D17** (1978)2298, Phys. Rev. **D19** (1979)2018.
7. MARK II Collab., D. Schlatter *et al.*, Phys. Rev. Lett. **49** (1982) 521;
   PLUTO Collab., Ch. Berger *et al.*, Z. Phys. **C12** (1982) 297;
   CELLO Collab., H.-J. Behrend *et al.*, Z. Phys. **C14** (1982) 95;
   MARKJ Collab., B. Adeva *et al.*, Phys. Rev. Lett. **50** (1983) 2051;
   JADE Collab., W. Bartel *et al.*, Z. Phys. **C25** (1984) 231;
   CELLO Collab., H.-J. Behrend *et al.*, Phys. Lett. **B138** (1984) 311;
   TASSO Collab., M. Althoff *et al.*, Z. Phys. **C26** (1984) 157;
   MAC Collab., E. Fernandez *et al.*, Phys. Rev. **D31** (1985) 2724;
   MARKJ Collab., B. Adeva *et al.*, Phys. Rev. Lett. **54** (1985) 1750;
   TASSO Collab., W. Braunschweig *et al.*, Z. Phys. **C36** (1987) 349;
   MARK II Collab., D.R. Wood *et al.*, Phys. Rev. **D37** (1988) 3091;
   TOPAZ Collab., I. Adachi *et al.*, Phys. Lett. **B227** (1989) 495;
   AMY Collab., H. Sagawa *et al.*, KEK Preprint 90-67 (1990).
8. ALEPH Collab., D. Decamp *et al.*, Phys. Lett. **B257** (1991) 479.
9. DELPHI Collab., P. Abreu *et al.*, Phys. Lett. **B252** (1990) 149.
10. L3 Collab., B. Adeva *et al.*, Phys. Lett. **B257** (1991) 469.
11. OPAL Collab., M.Z. Akrawy *et al.*, Phys. Lett. **B252** (1990) 159.
12. OPAL Collab., P.D. Acton *et al.*, Phys. Lett. **B276** (1992) 547.
13. SLD Collab., 'Measurements of Hadronic Decays of Z^0 Bosons', paper contributed to this conference and talk presented by D. Muller.
14. SLD Collab., talks presented at this conference by C. Damerell and J. Va'Vra.
15. SLD LAC Collab., SLAC-Pub-5354 (1992) (in preparation).
16. A.C. Benvenuti *et al.*, Nucl. Instr. Meth. **A290** (1990) 353.
17. S.C. Berridge *et al.*, Proceedings of the 1991 Nuclear Science Symposium, Santa Fe, NM, vol. 1, page 495; SLAC-Pub-5694 (1991) (to be published in IEEE Trans. Nucl. Sci.).

18. D.G. Richards, W.J. Stirling and S.D. Ellis, Nucl. Phys. **B229** (1983) 317.
19. A. Ali and F. Barreiro, Nucl. Phys. **B236** (1984) 269.
20. N.K. Falck and G. Kramer, Z. Phys. **C42** (1989) 459.
21. Z. Kunszt and P. Nason, Z Physics at LEP 1, CERN Report CERN 89-08, Vol. 1 eds. G. Altarelli, R. Kleiss and C. Verzegnassi, p. 373.
22. Review of Particle Properties, Phys. Rev. **D45** (1992) III.54.
23. G. Grunberg, Phys. Lett. **B95** (1980) 70.
24. P.M. Stevenson, Phys. Rev. **D23** (1981) 2916.
25. S.J. Brodsky, G.P. Lepage and P.B. Mackenzie, Phys. Rev. **D28** (1983) 228.
26. S. Sanghera, PRINT-92-0253 (CARLETON) (1992).
27. T. Sjöstrand and M. Bengtsson, Comp. Phys. Comm. **39** (1986) 347, Comp. Phys. Comm. **43** (1987) 367.
28. G. Marchesini et al., Comp. Phys. Comm. **67** (1992) 465.
29. TASSO Collab, W. Braunschweig *et al.*, Z. Phys. **C41** (1988) 359; P. N. Burrows, Z. Phys. **C41** (1988) 375.
30. OPAL Collab., M.Z. Akrawy *et al.*, Z. Phys. **C47** (1990) 505.
31. B.R. Webber, private communications.
32. SLD Collab., 'A Study of Jet Rates and Measurement of α_s at the Z^0 Resonance', paper contributed to this conference.

FIGURE CAPTIONS

Figure 1.

Vertical section in the plane including the $e^{\pm}$ beams of one quadrant of the SLD.

Figure 2.

Preliminary measured (a) *EEC* and (b) *AEEC* distributions at the detector level. The solid histograms represent the results from the JETSET 6.3 parton shower Monte Carlo program with initial state photon radiation, followed by SLD detector simulation, and the same event reconstruction program and analysis cuts as used for the real data. The dashed histograms show the corresponding results for the HERWIG 5.3 parton shower program.

Figure 3.

Correction factors $C_{det}(\chi_i)$ for detector effects and initial state photon radiation effects determined using JETSET 6.3.

Figure 4.

Correction factors $C_{frag}(\chi_i)$ for hadronization effects determined using JETSET 6.3.

Figure 5.

Preliminary results of the fits of $\mathcal{O}(\alpha_s^2)$ QCD to the measured (a) *EEC* and (b) *AEEC* distributions. The data were corrected to the parton-level by the JETSET 6.3 Monte C[illegible] program. Solid lines represent the $\mathcal{O}(\alpha_s^2)$ QCD predictions of KN with (a)$\Lambda_{\overline{MS}}$= [illegible]MeV and (b)$\Lambda_{\overline{MS}}$=119MeV for f=0.1.

Figure 6.

Preliminary results of fitted $\Lambda_{\overline{MS}}$ values as a function of the renormalization scale factor f for the RSE, AB, FK and KN formulae from (a)*EEC* and (b)*AEEC*. The error bar indicates the size of the statistical error.

Figure 7.

Preliminary results of $\alpha_s(M_Z)$ for (a)*EEC* and (b)*AEEC* from our analysis compared with those from similar LEP analyses. Error bars with solid lines indicate the experimental errors which include statistical and systematic errors; dashed lines indicate the theoretical errors. No $\alpha_s(M_Z)$ values are available from DELPHI for the *EEC* or from ALEPH for the *AEEC* in their papers.

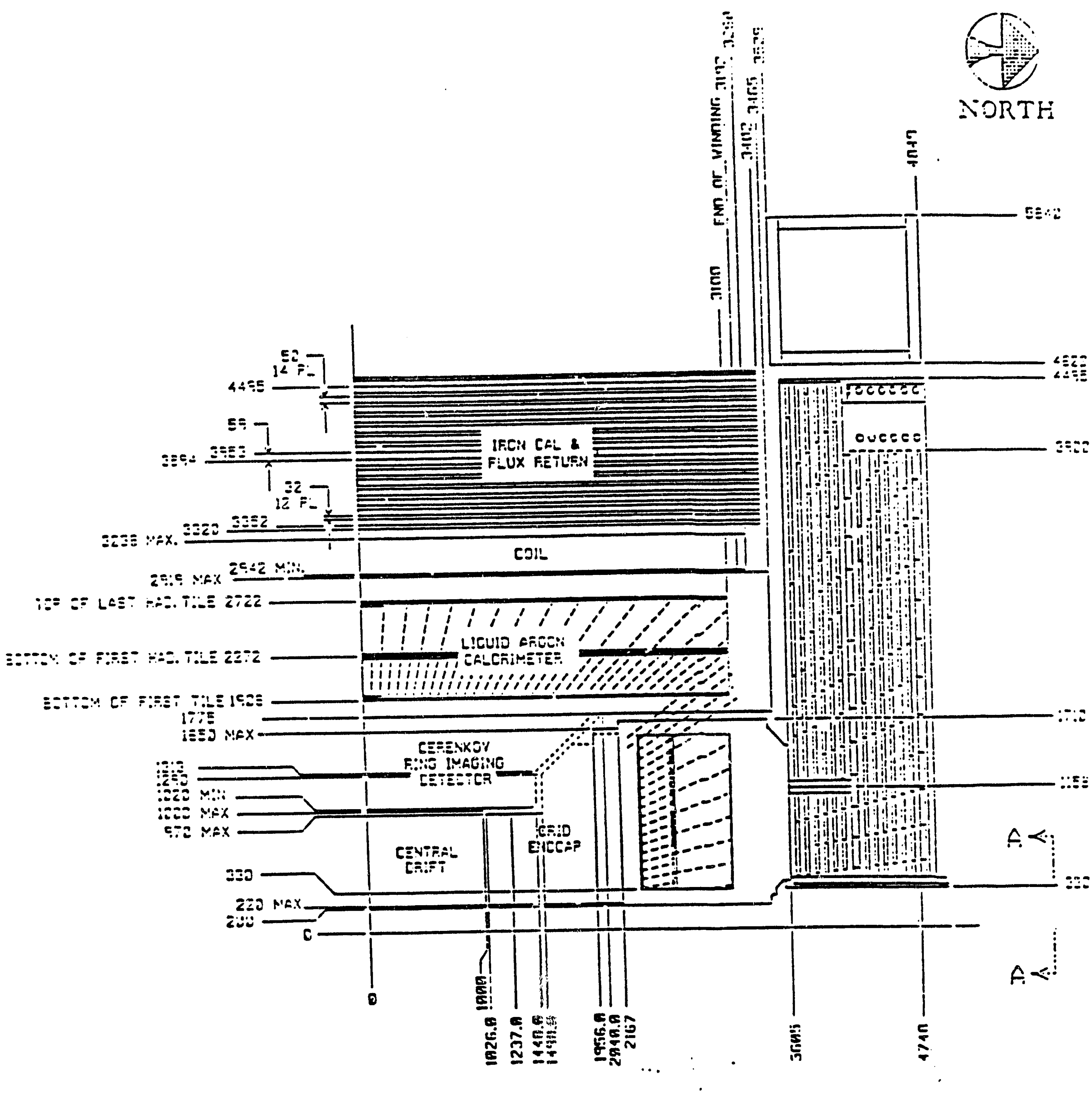
NORTH
IRON CAL &
FLUX RETURN
COIL
LIQUID ARGON
CALORIMETER
CERENKOV
RING IMAGING
DETECTOR
CENTRAL
DRIFT
GRID
ENDCAP
TOP OF LAST HAD. TILE 2722
BOTTOM OF FIRST HAD. TILE 2272
BOTTOM OF FIRST TILE 1928
1650 MAX
220 MAX
200
0
END OF WINDING
1026.0
1237.0
1956.0
2167
4740

Figure 1

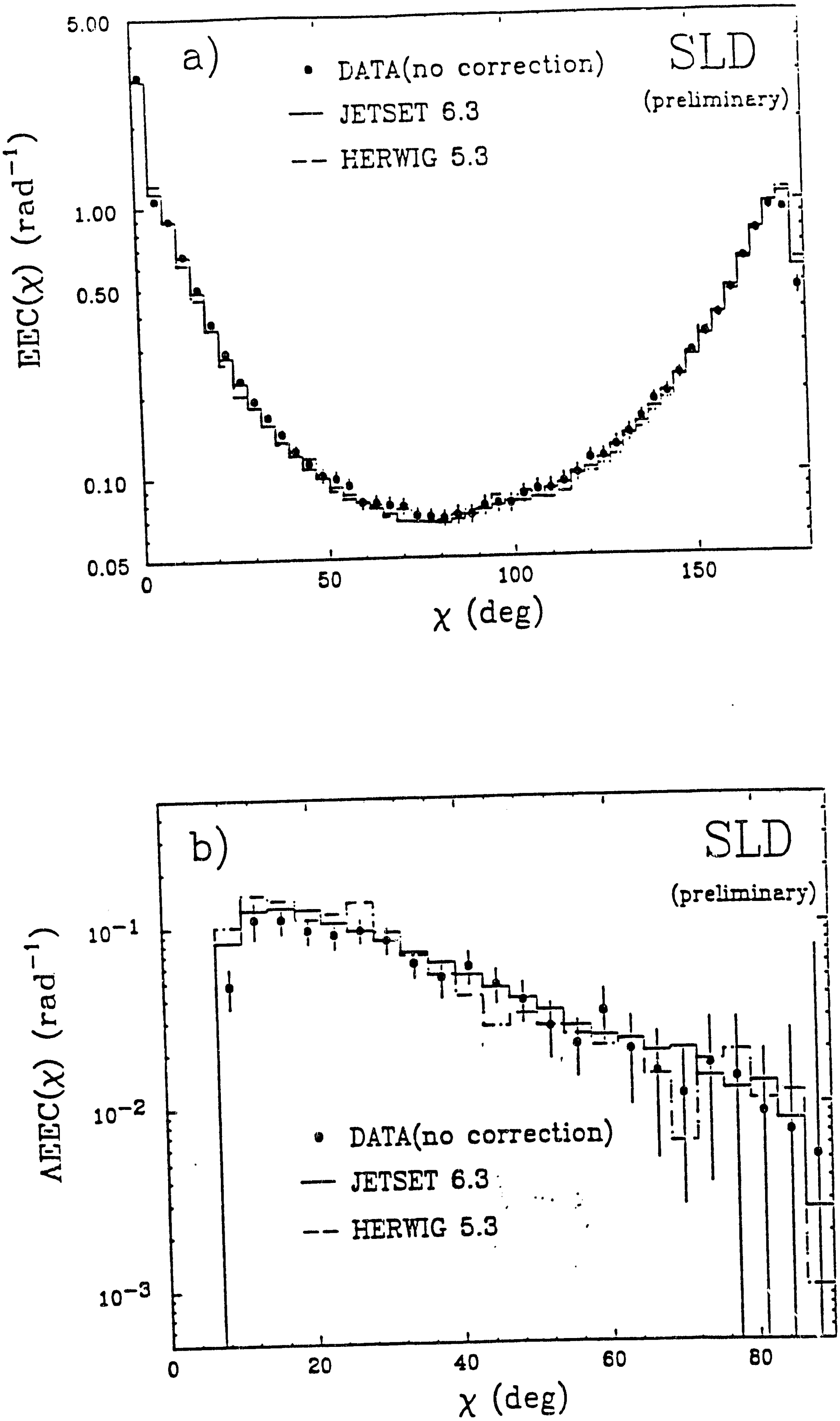
a)
DATA(no correction)
JETSET 6.3
HERWIG 5.3
SLD
(preliminary)
EEC(χ) (rad⁻¹)
5.00
1.00
0.50
0.10
0.05
0
50
100
150
χ (deg)
b)
SLD
(preliminary)
AEEC(χ) (rad⁻¹)
10⁻¹
10⁻²
10⁻³
DATA(no correction)
JETSET 6.3
HERWIG 5.3
0
20
40
60
80
χ (deg)

Figure 2

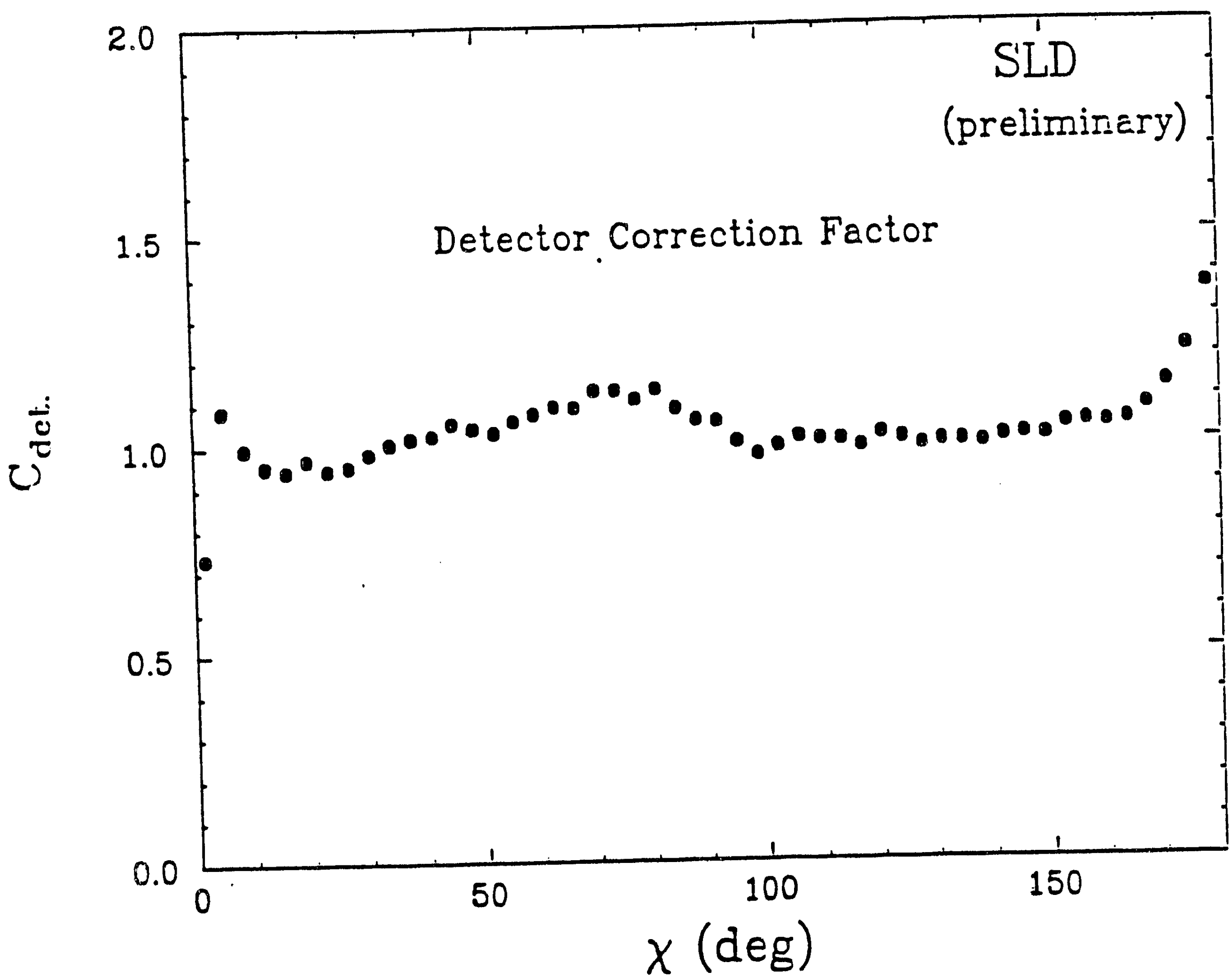
SLD
(preliminary)
Detector Correction Factor
2.0
1.5
1.0
0.5
0.0
$C_{det.}$
0
50
100
150
χ (deg)

Figure 3

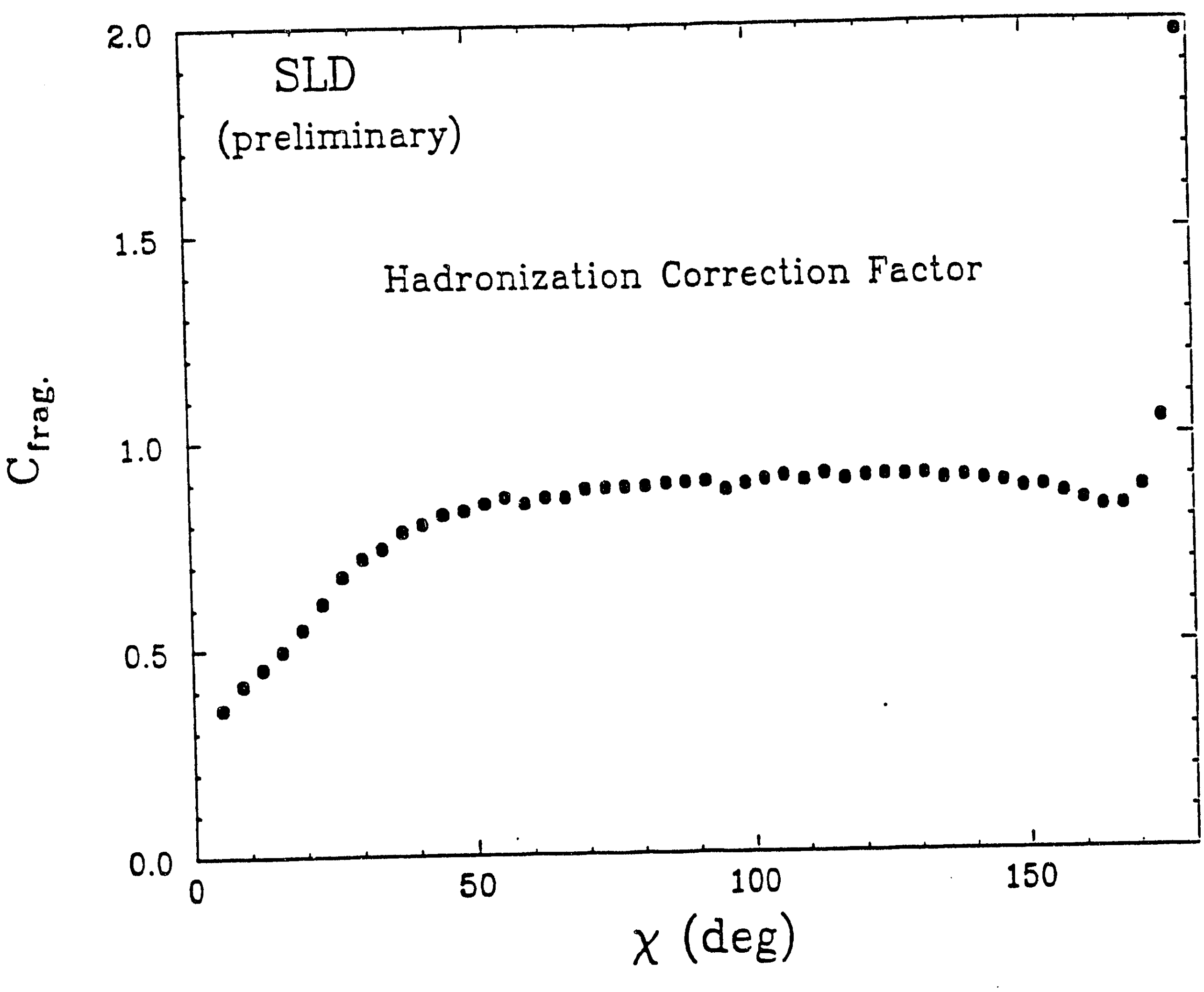

SLD
(preliminary)
Hadronization Correction Factor
$C_{frag.}$
2.0
1.5
1.0
0.5
0.0
0
50
100
150
χ (deg)

Figure 4

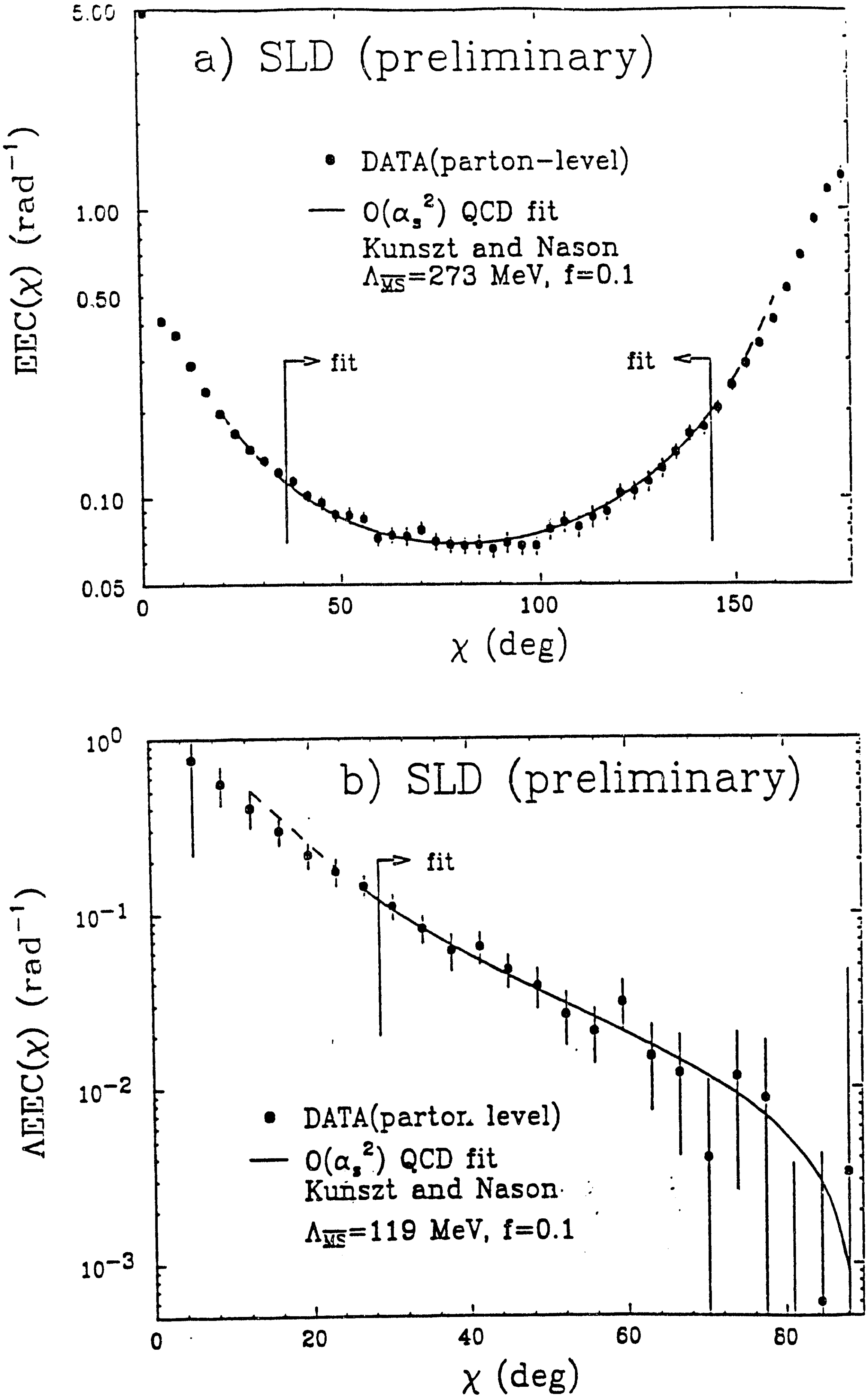
a) SLD (preliminary)
DATA(parton-level)
$O(\alpha_s^2)$ QCD fit
Kunszt and Nason
$\Lambda_{\overline{MS}}$=273 MeV, f=0.1
fit
fit
EEC(χ) (rad⁻¹)
χ (deg)
5.00
1.00
0.50
0.10
0.05
0
50
100
150
b) SLD (preliminary)
fit
DATA(parton level)
$O(\alpha_s^2)$ QCD fit
Kunszt and Nason
$\Lambda_{\overline{MS}}$=119 MeV, f=0.1
AEEC(χ) (rad⁻¹)
χ (deg)
10^0
10^{-1}
10^{-2}
10^{-3}
0
20
40
60
80

Figure 5

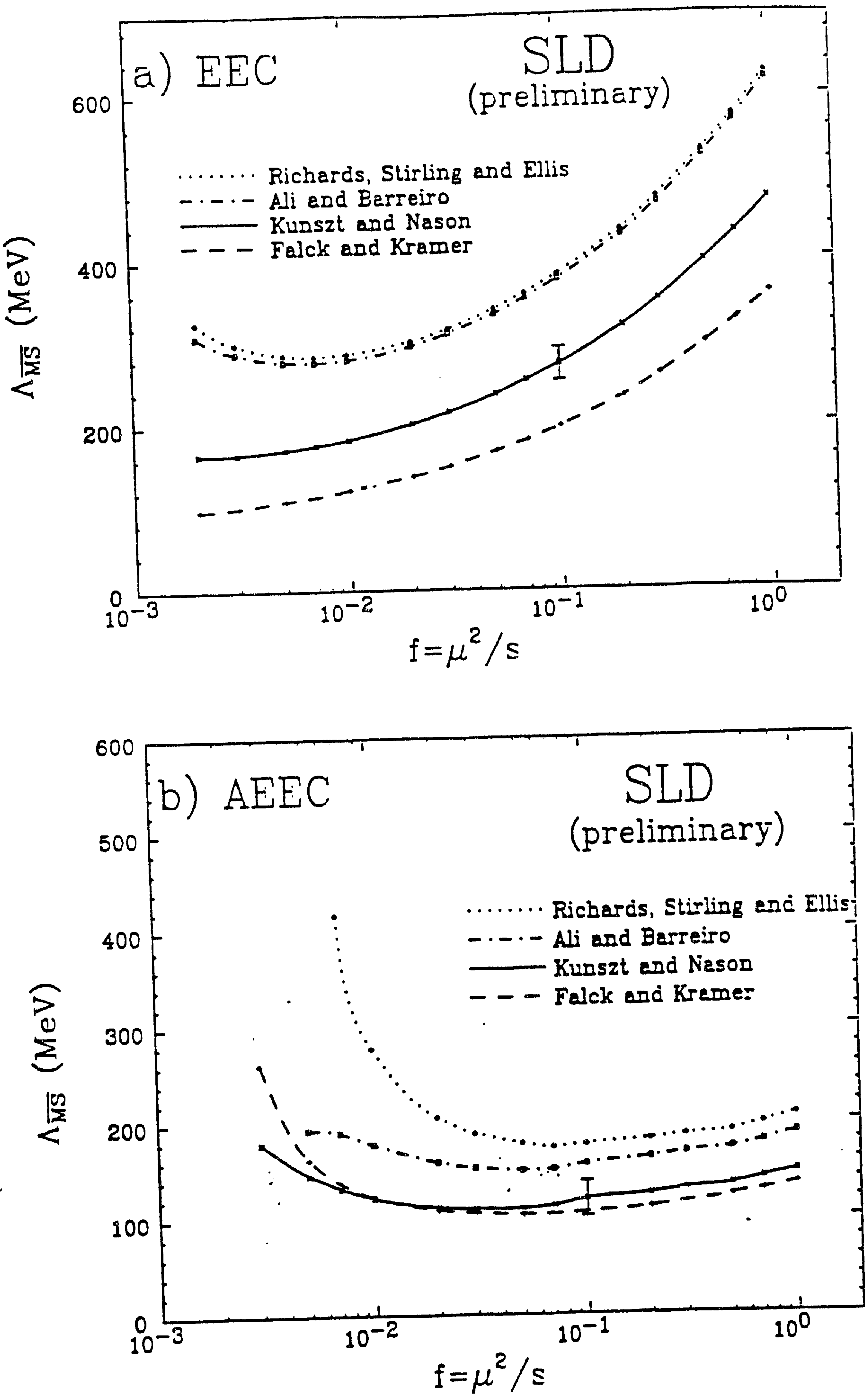

a) EEC
SLD
(preliminary)
Richards, Stirling and Ellis
Ali and Barreiro
Kunszt and Nason
Falck and Kramer
$\Lambda_{\overline{MS}}$ (MeV)
$f=\mu^2/s$
b) AEEC
SLD
(preliminary)
Richards, Stirling and Ellis
Ali and Barreiro
Kunszt and Nason
Falck and Kramer
$\Lambda_{\overline{MS}}$ (MeV)
$f=\mu^2/s$

Figure 6

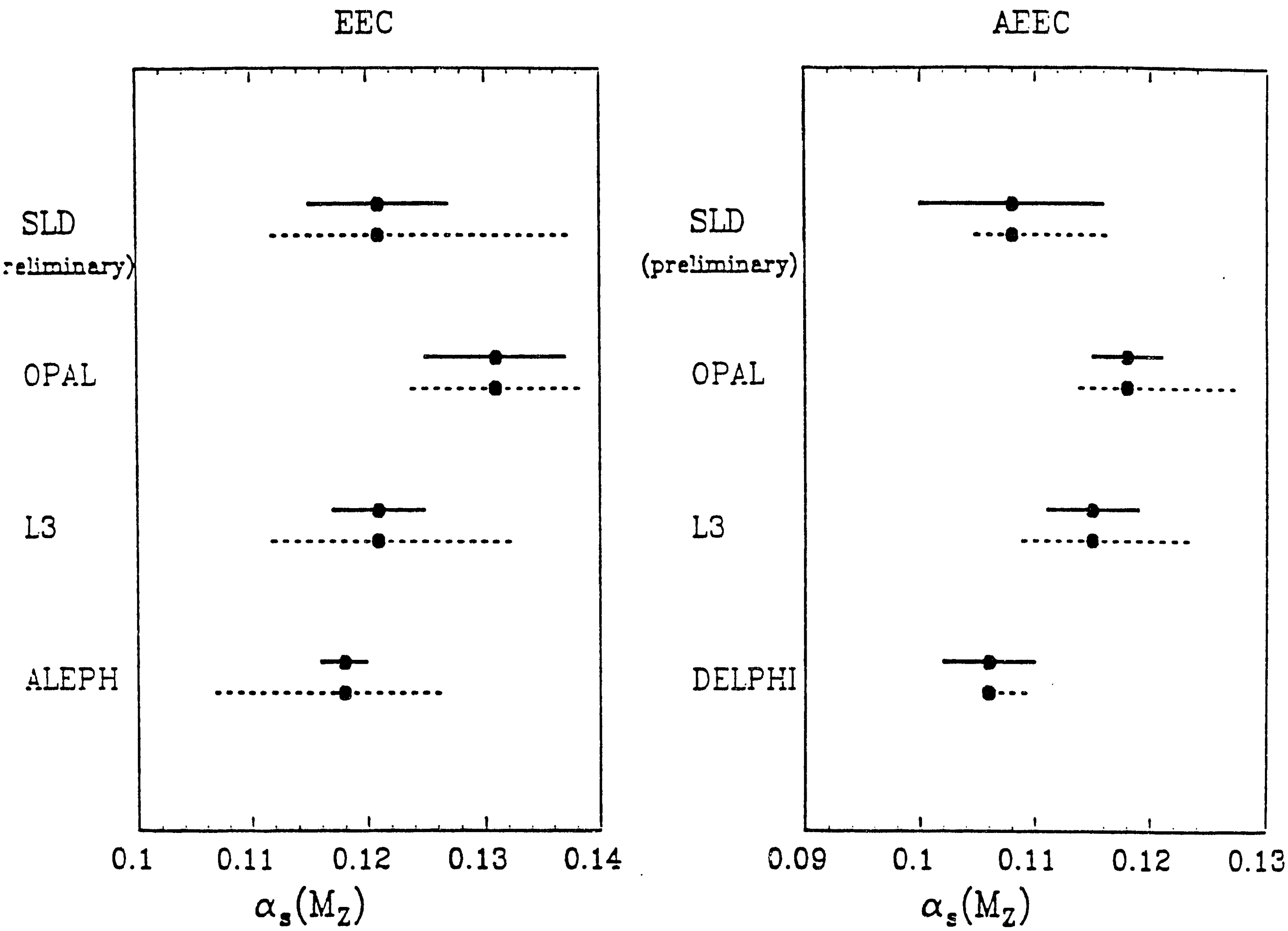
EEC
AEEC
SLD
reliminary)
(preliminary)
OPAL
L3
ALEPH
DELPHI
0.1
0.11
0.12
0.13
0.14
0.09
$\alpha_s(M_Z)$

Figure 7

DATE FILMED

3 / 15 / 93